Submitted to *Operations Research*
manuscript (Please, provide the mansucript number!)

Aggregate diffusion dynamics in agent-based models with a spatial structure

Gadi Fibich
Department of Applied Mathematics, Tel Aviv University, Tel Aviv 69978, Israel fibich@tau.ac.il

Ro'i Gibori
Department of Applied Mathematics, Tel Aviv University, Tel Aviv 69978, Israel gibori@platonix.com

We calculate explicitly the aggregate diffusion dynamics in one-dimensional agent-based models of adoption of new products, without using the mean-field approximation. We then introduce a clusters-dynamics approach, and use it to derive an analytic approximation of the aggregate diffusion dynamics in multi-dimensional agent-based models. The clusters-dynamics approximation shows that the aggregate diffusion dynamics does not depend on the average distance between individuals, but rather on the expansion rate of clusters of adopters. Therefore, the grid dimension has a large effect on the aggregate adoption dynamics, but a small-world structure and heterogeneity among individuals have only a minor effect. Our results suggest that the one-dimensional model and the Bass model provide a lower-bound and an upper-bound, respectively, for the aggregate diffusion dynamics in agent-based models with "any" spatial structure.

Key words: agent-based model, cellular automata, Bass model, diffusion, new products, small-world, mean-field approximation, heterogeneity

History:

1. Introduction

Diffusion of new products is a fundamental problem in Marketing. This problem has been studied in diverse areas such as retail service, industrial technology, agriculture, and educational, pharmaceutical and consumer-durables markets (Mahajan, Muller and Bass 1993). Typically, the diffusion process begins when the product is introduced into the market, and progresses through a series of adoption events.

The first quantitative model of diffusion of new products was the Bass model (Bass 1969). This model inspired a huge body of theoretical and empirical research, and was selected as one of the ten most cited papers in the 50-year history of Management Science (Management

Science 2004). In the Bass model, the adoption rate is given by

$$\frac{\mathrm{d}n(t)}{\mathrm{d}t} = [M - n(t)][p + \frac{q}{M}n(t)], \qquad n(0) = 0, \tag{1}$$

where $n(t)$ is the number of individuals that adopted the product by time t, and M is the population size. The parameters p and q describe the likelihood of an individual to adopt the product due to *external influences* such as mass-media or commercials, and due to *internal influences* by other individuals who have already adopted the product, respectively. Since the *hazard of adoption* of each individual is $p + q\frac{n}{M}$, each individual is affected by both external and internal influences.

Equation (1) can be solved explicitly, yielding

$$n_{\mathrm{Bass}}(t) = M\frac{1 - e^{-(p+q)t}}{1 + \frac{q}{p}e^{-(p+q)t}},$$

or, equivalently,

$$f_{\mathrm{Bass}}(t) = \frac{1 - e^{-(p+q)t}}{1 + \frac{q}{p}e^{-(p+q)t}}, \tag{2}$$

where $f(t) = n(t)/M$ is the fraction of adopters at time t. Empirically, the Bass model was found to capture the S-shape of the adoption curve of various products. Typical values for the parameters were found to be $p = 0.03$/year and $q = 0.38$/year, with p often less than 0.01/year and q typically in the range 0.3–0.5/year (Mahajan, Muller and Bass 1995).

The Bass model is an aggregate model, i.e., it describes the diffusion in terms of the behavior of the entire population. Therefore, a considerable research effort has been devoted to model the individual adoption behavior, and to analyze how it affects the aggregate diffusion process. Thus, Sinha and Chandrashekaran (1992) studied individual adoption behavior using hazard modeling on empirical data. Subsequently, Van den Bulte and Lilien (2001) used hazard modeling to study social contagion with social network data. Bronnenberg and Mela (2004) and Bell and Song (2007) have done this with spatial data. Beginning with Goldenberg et al. (2000), this line of research has been carried out by using agent-based (cellular-automata) models to

Figure 1 The Fully-Connected model. Each individual is able to communicate with any other individual.

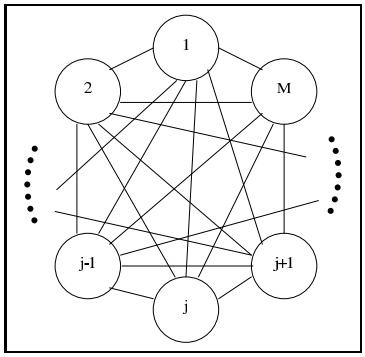

compute *numerically* the aggregate adoption curve from the individual-based behaviors, which are based on external and internal effects.

In the Bass model, the rate of new adoptions due to internal effects is equal to $\frac{q}{M}(M-n)n$. This expression is based on the assumption that each of the $(M-n)$ non-adopters can be influenced by all n adopters. In other words, the Bass model implicitly assumes that all individuals are connected to each other (see Figure 1). The assumption of a *full connectivity* has also been used in some of the subsequent agent-based diffusion models. For example, Goldenberg, Libai and Muller (2001) used a fully-connected agent-based model to study the effect of heterogeneity in the values of p and q among individuals. In other agent-based diffusion models, however, individuals could only communicate with their neighbors, and the population had a spatial structure such as a one-dimensional grid (e.g., Alkemade and Castaldi (2005)), a two-dimensional grid (e.g., Goldenberg, Libai and Muller (2002)), or a regular lattice with some added random links (e.g., Garber et al. (2004), Delre et al. (2007)).

The goal of this study is to study *analytically* the effect of the spatial structure on the diffusion process in agent-based models. To do that, we first consider a one-dimensional model in which each individual can only be influenced by one or two neighbors (see Figure 2). In this case, we show that the fractional adoption curve $f_{1D}(t)$ can be calculated explicitly, without making any approximation. In particular, as $M \longrightarrow \infty$,

$$f_{1D}(t) = 1 - e^{-(p+q)t+q\frac{1-e^{-pt}}{p}}. \tag{3}$$

Figure 2 The 1D diffusion models analyzed in this study. Arrows show the possible flow of communication/influence. A: The one-sided 1D model. Each individual can be influenced by his left neighbor. B: The two-sided 1D model. Each individual can be influenced by his two neighbors.

We then introduce a novel analytic approach, the *clusters-dynamics method*, which allows us to approximate the adoption curve in higher dimensions when all nodes are "positionally equivalent" to each either, with and without an additional small-world structure. The key finding of this study is that the fractional adoption curve $f(t)$ in an agent-based model with "any" spatial structure is slower than in the Bass model and faster than in the 1D model, i.e.,

$$f_{\text{Bass}}(t) \leq f(t) \leq f_{\text{1D}}(t). \tag{4}$$

The paper is organized as follows. In Section 2 we study the diffusion in the simplest possible spatial model, the *one-sided one-dimensional model*, in which a population of size M is positioned on a circle, and each individual can only be influenced by his left neighbor (see Figure 2A). Even for such a simple structure, the number of possible configurations of adopters and non-adopters increases exponentially with the length of the configuration. In such cases, the common approach to compute analytically the aggregate diffusion dynamics has been to calculate only the probabilities of short configurations, and close the system using the mean-field approximation (see, e.g., Matsuda et al. (1992)). In Section 2.2 we show, however, that we can close the system *without making any approximation*, by utilizing the translation invariance property of the model. Furthermore, this system of equations can be solved, yielding *an explicit expression of the aggregate diffusion dynamics* (Proposition 1). This expression is, however, cumbersome, and not very informative. Fortunately, it can be substantially simplified in the limit as $M \longrightarrow \infty$ (Proposition 2), yielding equation (3). Numerical simulations

show that already for M as small as 20, this limiting expression is in excellent agreement with simulation results of agents-based models. Since typical values of M are much larger, expression (3) provides an excellent approximation to the aggregate diffusion process in the one-sided one-dimensional spatial model.

In Section 3 we study the diffusion in a *two-sided one-dimensional model*, in which a population of size M is positioned on a circle, but each individual can influence his two neighbors (see Figure 2B). In this model, we allow for an asymmetry of the internal influence parameters in the right and left directions (i.e., q_R is not necessarily equal to q_L). We again utilize the translation invariance property to compute analytically the aggregate diffusion dynamics without making any mean-field approximation (Proposition 3), and obtain a simpler expression as $M \longrightarrow \infty$ (Proposition 4).

The results of Propositions 1 and 3 show that the aggregate diffusion dynamics in the one-sided 1D model is identical to that in the two-sided 1D model, provided that the internal influence parameter q in the one-sided model is equal to the sum of the internal influence parameters in the two-sided model (i.e., $q = q_R + q_L$). Therefore, in Section 4 we define the parameter $q^{\text{effective}}$ as the sum of the internal influences parameters on all neighbors. The results of Sections 2 and 3 thus show that *in the one-dimensional models, the aggregate diffusion dynamics depends on the values of* p *and* $q^{\text{effective}} = q_R + q_L$.

In Section 5 we show that as $M \longrightarrow \infty$, the adoption curve in the fully-connected model (see Figure 1) is given by the Bass formula, equation (2). Then, in Section 6 we show that the aggregate adoption level in the 1D model is significantly lower than in the Bass model. Since the Bass model can be viewed as a mean-field approximation of the 1D model (Section 6.1), this shows the advantage of using the translation invariance property over the mean-field approximation in the analytic calculation of the adoption curve in the 1D models.

The one-dimensional model and the fully-connected Bass model can be viewed as the least-connected and most-connected spatial models, respectively. From this perspective, any other

spatial structure "lies between" these two cases. Therefore, in Section 7 we formulate Conjecture 1 that *the diffusion in any spatial structure is faster than in the 1D model, and slower than in the Bass model*, see equation (4). In other words, the explicit expressions (2) and (3) provide an upper-bound and a lower-bound to the fractional adoption curve.

In general, the aggregate adoption dynamics depends on two independent parameters, p and q. In Section 8, however, we use dimensional analysis to show that regardless of the spatial structure, the adoption curve can be written as a function of a *single* parameter — the dimensionless parameter $\tilde{q} = q/p$. Moreover, we show that the domain of interest in diffusion models is $\tilde{q} \gg 1$. This observation implies that it is "sufficient" to prove Conjecture 1 (or to confirm it numerically) for $\tilde{q} \gg 1$, rather than for any $p > 0$ and $q > 0$.

In Section 9 we derive an approximation for $f(t)$, by visualizing the diffusion process as a random creation and subsequent expansion of clusters of adopters. Unlike the explicit calculation of $f(t)$ in the 1D models which utilized the translation invariance property, the clusters-dynamics approach only provides an approximation for $f(t)$. Nevertheless, it has the advantages that it is intuitive, and that it can be applied in any dimension. Indeed, using the cluster-dynamics approach, we show analytically that the aggregate adoption level in multidimensional Cartesian grids increases with the grid dimension, but remains below that of the Bass model (Section 10). A priori, one could argue that these results are not surprising, since as the dimension increases, the average distance between adopters decreases, thereby resulting in a faster diffusion. If this explanation is correct, then the addition of a small-world structure should result in a considerable speedup of the adoption process. In Section 11 we show, however, that a small-world structure has a small effect on the diffusion of new products. Indeed, a small-world structure has a large effect when diffusion starts from a single external adopter and progresses only through internal adoptions. This may be the case in diffusion of epidemics such as AIDS or SARS, but not in diffusion of new products. In Section 12 we use the clusters-dynamics approach and agent-based simulations to show that heterogeneity among individuals has a minor effect on the aggregate diffusion process.

The results of Sections 10–12 show, in particular, that Conjecture 1 holds for Cartesian grids of any dimension, with or without a small-world structure, with either homogeneous or heterogeneous individuals. The role of the spatial structure in the diffusion process is discussed in Section 13. The main conclusion of this discussion is that *the spatial structure can have a large effect on the diffusion process. This effect is not related to the effect of the spatial structure on the average distance between individuals, but rather to its effect on the expansion rate of clusters of adopters.* We conclude with some final remarks in Section 14.

While the focus of this study in on agent-based modeling in Marketing, we note that agent-based models have been used in studies of social, economical, and biological models (see, e.g., Samuelson and Macal (2006), Gilbert and Troitzsch (2005), Grimm and Railsback (2005), Bonabeau (2002), Epstein and Axtell (1996), Kim et al (2007)). From a mathematical perspective, the key novelty of this study, compared with the existing literature on agent-based models, is the *analytic* calculation of the aggregate diffusion *dynamics* in a grid with a spatial structure, both exactly for the 1D case, and approximately (using the clusters-dynamics approach) in any dimension. In contrast, most previous agent-based studies computed the aggregate diffusion dynamics only *numerically*. The studies that did calculate the aggregate dynamics analytically, either employed some type of a mean-field approximation, or obtained analytical results for steady-state solutions, such as the fraction of the population that will become infected by an epidemic at equilibria (López-Pintado 2008, Jackson and Rogers 2007, Jackson 2006, Vega-Redondo 2006, Pastor-Satorrás and Vespignani 2001). Note that in all the agent-based models considered in this study, once an individual becomes an adopter, he remains so at all later time. This assumption is reasonable in the product-innovation context, where diffusion models try to forecast first-purchase sales of innovations, such as fax machines, Skype, Ipod, and Facebook. In such models, one is only interested in the adoption *dynamics*, since the steady-state equilibria is for the entire population to become adopters.

2. One-sided 1D model

We begin with the simplest one-dimensional model, in which a population of size M is positioned on a circle, such that each individual can only be influenced by his left neighbor (see Figure 2A). We assume that at time $t=0$ no individual has adopted the product, and that once an individual adopts, he remains an adopter at all later times.

Assume that at time t individual j has not yet adopted. Let p be his adoption rate due to external influences, let q be his adoption rate due to internal influence from his left neighbor (provided that his left neighbor has already adopted), and let the probability that he adopts between times t and $t+\Delta t$ be given by

$$\text{Prob}\{j \text{ adopts in } (t,t+\Delta t)\} = \begin{cases} P_0\Delta t + o(\Delta t), & j-1 \text{ did not adopt by time } t, \\ P_1\Delta t + o(\Delta t), & \text{otherwise,} \end{cases} \tag{5a}$$

as $\Delta t \to 0$, where

$$P_0 = p, \qquad P_1 = p+q. \tag{5b}$$

Here and elsewhere we use the convention that when $j=1$, then $j-1$"="M.

Let us denote the number of adopters by $n(t)$. Then, we can calculate explicitly the expected fraction of adopters $f(t)=E[n(t)]/M$:

PROPOSITION 1. *The expected fraction of adopters in the one-sided 1D model is given by*

$$f(t) = 1 - \sum_{k=1}^{M-1} c_k \frac{(-q)^{k-1}}{p^{k-1}(k-1)!} e^{(-kp-q)t} \; + \; c_M \frac{(-q)^{M-1}}{\prod_{j=1}^{M-1}(jp-q)} e^{-Mpt}. \tag{6a}$$

Here, the constants $\{c_k\}_{k=1}^M$ *are the solutions of the linear system*

$$\sum_{k=1}^{M} c_k \mathbf{v_k} = \begin{pmatrix} 1 \\ \vdots \\ 1 \end{pmatrix}, \tag{6b}$$

where

$$\mathbf{v}_k = \begin{pmatrix} \big(-q\big)^{k-1}/\big(p^{k-1}(k-1)!\big) \\ \big(-q\big)^{k-2}/\big(p^{k-2}(k-2)!\big) \\ \vdots \\ \big(-q\big)/p \\ 1 \\ 0 \\ \vdots \\ 0 \end{pmatrix}, \quad k=1,\ldots,M-1; \qquad \mathbf{v}_M = \begin{pmatrix} \big(-q\big)^{M-1}/\prod_{j=1}^{M-1}\big(jp-q\big) \\ \big(-q\big)^{M-2}/\prod_{j=1}^{M-2}\big(jp-q\big) \\ \vdots \\ \big(-q\big)^2/\big(p-q\big)\big(2p-q\big) \\ \big(-q\big)/\big(p-q\big) \\ 1 \end{pmatrix}. \tag{6c}$$

Proof: see Section 2.2.

Although we obtained an explicit expression for the expected fraction of adopters, this expression is cumbersome and not very informative. Fortunately, as $M \to \infty$, this explicit expression becomes considerably simpler:

PROPOSITION 2. *The expected fraction of adopters in the one-sided 1D model as $M \to \infty$ is*

$$\lim_{M\to\infty} f(t) = 1 - e^{-(p+q)t+q\frac{1-e^{-pt}}{p}}. \tag{7}$$

Proof: see Section 2.3.

This expression for the expected fraction of adopters is different from the one obtained from the Bass model, see Section 6.

2.1. Simulations

In Figure 3 we show the average number of adopters, calculated from 10,000 agent-based simulations of the one-sided 1D model. For both $M = 10$ and $M = 20$, the average fraction of adopters is well approximated by the explicit expression (6) for a finite M. When $M = 10$ the average fraction of adopters is below the $M \to \infty$ limit, equation (7). However, already for $M = 20$, the average fraction of adopters is very close to the $M \to \infty$ limit. This shows that even for rather small populations, the $M \to \infty$ limit describes the adoption in the one-sided 1D model extremely well.

The results shown in Figure 3 are the average of 10,000 agents-based simulations. Note, however, that as $M \longrightarrow \infty$, the normalized variance of the adoption process goes to zero. Hence,

Figure 3 Fraction of adopters as a function of time in the one-sided 1D model, as calculated from agent-based simulations which are averaged over 10,000 runs (dashes). Also shown are the explicit expression (6) for a finite M (dots), and the explicit expression (7) for an infinite population (solid). Here, $p=0.01$, $q=0.6$ and $\Delta t=0.05$. (A) $M=10$. Dashed and dotted lines are indistinguishable. (B) $M=20$. All three lines are indistinguishable.

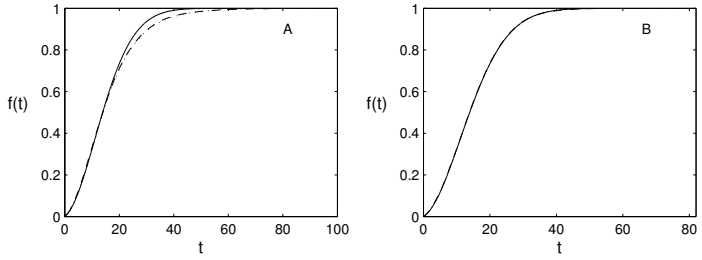

Figure 4 Fraction of adopters as a function of time in the one-sided 1D model, as calculated from a *single* agent-based simulation (dashes). Also shown is the explicit expression (7) for an infinite population (solid). Here, $p=0.01$, $q=0.6$ and $\Delta t=0.05$. (A) $M=100$, (B) $M=10^6$. In B, the two lines are indistinguishable.

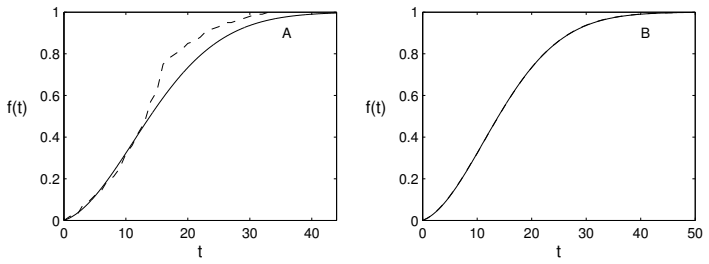

the $M\longrightarrow\infty$ limit, equation (7), will match any simulation result and not just the average over many simulations. To illustrate this, in Figure 4 we compare the $M\longrightarrow\infty$ limit with a *single* agent-based simulation. When $M=100$, there is a considerable difference between the two cases. When $M=10^6$, however, the two cases are indistinguishable.

2.2. Proof of Proposition 1

We denote the state of individual j by the random variable $X_j(t)$, where $X_j(t)=0$ if j has not adopted by time t, and $X_j(t)=1$ if j has adopted by time t. Since at time $t=0$ no one has adopted,

$$X_j(0)=0, \qquad j=1,\ldots,M. \tag{8}$$

Recall that once $X_j(t)$ changes to 1, it remains so at all later times.

Using the adoption probabilities in equation (5a), we calculate the following conditional probabilities:

$$\begin{aligned}
&\text{Prob}\big\{X_j(t+\Delta t)=1|X_j(t)=1\big\}=1,\\
&\text{Prob}\big\{X_j(t+\Delta t)=1|X_{j-1}(t)=0,X_j(t)=0\big\}=P_0\Delta t+o(\Delta t),\\
&\text{Prob}\big\{X_j(t+\Delta t)=1|X_{j-1}(t)=1,X_j(t)=0\big\}=P_1\Delta t+o(\Delta t).
\end{aligned} \tag{9}$$

Therefore,

$$\begin{aligned}
\text{Prob}\big\{X_j(t+\Delta t)=1\big\}=\text{Prob}\big\{X_j(t)=1\big\}\cdot 1 \;+\; \text{Prob}\big\{X_{j-1}(t)=0,X_j(t)=0\big\}\cdot\Big(P_0\Delta t+o(\Delta t)\Big)\\
+\;\text{Prob}\big\{X_{j-1}(t)=1,X_j(t)=0\big\}\cdot\Big(P_1\Delta t+o(\Delta t)\Big).
\end{aligned}$$

Taking the limit as Δt goes to zero gives

$$\frac{\mathrm{d}}{\mathrm{d}t}\text{Prob}\big\{X_j(t)=1\big\}=P_0\cdot\text{Prob}\big\{X_{j-1}(t)=0,X_j(t)=0\big\}+P_1\cdot\text{Prob}\big\{X_{j-1}(t)=1,X_j(t)=0\big\}. \tag{10}$$

In order to proceed we adopt the following notations. We denote the probability of an individual j to be in state 'I' (infected) at time t by $[\underline{I}]$. We denote the probability of individual j to be in state 'S' (susceptible) at time t by $[\underline{S}]$. The position of individual j (the "*anchor*") in these configurations is underlined. The probability of a larger configuration that includes individual j at time t is denoted accordingly. For example, the probability of $j-1$ and j to be in state 'SS' at time t is $[S\underline{S}]$, etc. We denote a configuration with parentheses, so that $(S\underline{S})$ is the configuration and $[S\underline{S}]$ is the probability of that configuration.

Using this notation, equation (10) can be rewritten as

$$[\dot{\underline{I}}]=P_0[S\underline{S}]+P_1[I\underline{S}], \tag{11}$$

where the dot stands for time differentiation. This equation is referred to as the *master equation for* $[\underline{I}]$, and it describes the time evolution of $[\underline{I}]$ given the probabilities $[S\underline{S}]$ and $[I\underline{S}]$.

2.2.1. Translation Invariance

Equation (11) is not closed, since it is a single equation with three unknown state variables. In order to have a closed system of equations, we need to derive the master equations for $[S\underline{S}]$ and $[I\underline{S}]$. These equations, however, depend on the probabilities of various configurations of length 3, whose master equations depend on configurations of length 4, etc. Since the number of configurations increases exponentially with the length of the configurations, it seems that even writing down the entire system of equations is a formidable task. In such cases, a common approach is to calculate only the probabilities of short configurations and close the system using some mean-field approximation (see, e.g., Matsuda et al. (1992)). We now show that in the one-sided 1D model it is possible to close the system without making any approximation, by utilizing the translation invariance property of the diffusion process.

LEMMA 1. *The adoption process in the one-sided 1D model is translation invariant, i.e., the probability of each configuration does not depend on its position. In other words, for any k,*

$$Prob\big\{X_j(t)=\sigma_j,\ldots,X_r(t)=\sigma_r\big\}=Prob\big\{X_{j+k}(t)=\sigma_j,\ldots,X_{r+k}(t)=\sigma_r\big\}, \tag{12}$$

where each σ_k is either 0 or 1.

Proof. The initial condition (8) is the same for all j, and the adoption rate (5) does not depend on the position of the individual. □

Therefore,

COROLLARY 1. *The position of the "anchor" in the configuration does not affect the probability of that configuration.*

Thus, for example $[\underline{S}IS]=[S\underline{I}S]=[SI\underline{S}]$. In particular, $[\underline{I}]=[I]$.

LEMMA 2.

$$[I]=f(t). \tag{13}$$

Proof. The number of adopters at time t is $n(t)=\sum_{j=1}^{M}X_j(t)$. Therefore, the expected number of adopters at time t is

$$E\big[n(t)\big]=E\big[\sum_{j=1}^{M}X_j(t)\big]=\sum_{j=1}^{M}E\big[X_j(t)\big]=\sum_{j=1}^{M}\mathrm{Prob}\big\{X_j(t)=1\big\}.$$

From translation invariance, we have $[I] = \text{Prob}\{X_j(t) = 1\}$ for all j, which gives (13). □

2.2.2. Larger Configurations

Let us denote by (S_k) a configuration that consists of a sequence of k adjacent non-adopters, i.e.,

$$(S_k) = (\underbrace{\underline{S} \dots \underline{S}}_{k \text{ times}}).$$

We have the following result:

LEMMA 3.

$$[IS_k] = [S_k] - [S_{k+1}]. \tag{14}$$

Proof. The configuration $(S_k) = (S_{k-1}\underline{S})$ may be written as a union of two disjoint configurations

$$(S_{k-1}\underline{S}) = (SS_{k-1}\underline{S}) \cup (IS_{k-1}\underline{S}).$$

Therefore, its probability is the sum of the probabilities of the disjoint configurations:

$$[S_k] = [S_{k+1}] + [IS_k].$$

□

We now derive the master equation of any (S_k) configuration:

LEMMA 4. *The master equation for* $[S_k]$ *is*

$$[\dot{S}_k] = \Big(- kp - q\Big)[S_k] + q[S_{k+1}], \qquad k = 1, \dots, M-1. \tag{15}$$

Proof. A configuration $(S_{k-1}\underline{S})$ cannot be created, as the only possible transformation is an 'S' becoming an 'I'.

A configuration $(S_{k-1}\underline{S})$ is destroyed on the $k+1$ occasions:

1. When any of the rightmost $k-1$ 'S's in a configuration $(S_{k-1}\underline{S})$ turns into an 'I', which happens at a rate of P_0.

2. When a configuration $(SSS_{k-2}\underline{S})$ transforms into the configuration $(SIS_{k-2}\underline{S})$, which happens at a rate of P_0.

3. When a configuration $(ISS_{k-2}\underline{S})$ transforms into the configuration $(IIS_{k-2}\underline{S})$, which happens at a rate of P_1.

The master equation for $[S_k]$ is therefore

$$[\dot{S_k}] = -(k-1)P_0[S_k] - P_0[S_{k+1}] - P_1[IS_k].$$

Substituting (5b) and (14) gives (15). □

LEMMA 5. *The master equation for* $[S_M]$ *is:*

$$[\dot{S_M}] = -Mp[S_M]. \tag{16}$$

Proof. A configuration (S_M) cannot be created, as the only possible transformation is an 'S' becoming an 'I'. A configuration (S_M) is destroyed when any of the M 'S's turns into an 'I', which happens at a rate of $P_0 = p$. The master equation for $[S_M]$ is therefore given by (16). □

Combining equations (15) and (16) shows that the time evolution of $\{[S_k]\}_{k=1}^{M}$ is given by

$$[\dot{\mathbf{S}}] = \mathbf{A}[\mathbf{S}], \tag{17a}$$

together with the initial condition

$$[\mathbf{S}]_{|t=0} = \begin{pmatrix} 1 \\ \vdots \\ 1 \end{pmatrix}, \tag{17b}$$

where

$$[\mathbf{S}] = \begin{pmatrix} [S_1] \\ \vdots \\ [S_M] \end{pmatrix}, \qquad [\dot{\mathbf{S}}] = \begin{pmatrix} [\dot{S_1}] \\ \vdots \\ [\dot{S_M}] \end{pmatrix}, \qquad \mathbf{A} = \begin{pmatrix} -p-q & q & 0 & 0 & \dots & \dots & 0 \\ 0 & -2p-q & q & 0 & \ddots & \ddots & \ddots \\ 0 & 0 & -3p-q & q & \ddots & \ddots & \ddots \\ \vdots & \ddots & 0 & \ddots & \ddots & \ddots & 0 \\ \vdots & \ddots & 0 & \ddots & -kp-q & q & 0 \\ \vdots & \ddots & \ddots & \ddots & \ddots & \ddots & q \\ 0 & \ddots & \ddots & \dots & 0 & 0 & -Mp \end{pmatrix}.$$

Equation (17) is a system of linear, constant-coefficients ordinary differential equations, which can be explicitly solved as follows. The eigenvalues of $\mathbf{A}$ are its diagonal elements, i.e.,

$$\lambda_k = \begin{cases} -kp - q, & k = 1, \ldots, M-1, \\ -Mp, & k = M. \end{cases}$$

The corresponding eigenvectors $\{\mathbf{v}_k\}_{k=1}^M$ are given by equation (6c). Therefore, the solution of equation (17) is given by

$$[\mathbf{S}] = \sum_{k=1}^{M} c_k \mathbf{v_k} e^{\lambda_k t}.$$

The coefficients $\{c_k\}_{k=1}^M$ are determined from the initial condition (17b), hence are given in equation (6b). Since $E\big[f(t)\big] = [I] = 1 - [S_1]$, this concludes the proof of Proposition 1.

2.3. Proof of Proposition 2

We first note that when $M = \infty$, the solution of the infinite system of ODEs (17) is given by

$$[S_k] = e^{-(k-1)pt}[S_1], \qquad k = 1, 2, \ldots \tag{18}$$

Indeed, substituting (18) in (15) yields

$$\Big(-(k-1)p\Big)e^{-(k-1)pt}[S_1] + e^{-(k-1)pt}[\dot{S}_1] = \Big(-kp - q\Big)e^{-(k-1)pt}[S_1] + qe^{-kpt}[S_1],$$

or after some rearranging,

$$[\dot{S}_1] = -(p+q)[S_1] + qe^{-pt}[S_1].$$

The solution of this equation with the initial condition $[S_1]_{|t=0} = 1$ is given by equation (7). □

Remark: A system of differential equations similar to equations (17) was derived by Alfrey and Lloyd (1963) in a model of the accumulation of gas or liquid molecules on the surface of a solid, as they form long molecular films. Our solution for $M = \infty$ is similar to the one found by Keller (1963) for that problem.

3. Two-sided 1D model

In this section we analyze a 1D model in which a population of size M is positioned on a circle, and each member of the population can communicate with his two neighbors (see Figure 2B). Let p be his adoption rate due to external influences, let q_L be his adoption rate due to internal influence from his left neighbor if he has already adopted, let q_R be his adoption rate due to internal influence from his right neighbor if he has already adopted, and let the overall adoption probability be given by

$$\text{Prob}\{j \text{ adopts in } (t,t+\Delta t)\} = \begin{cases} P_0\Delta t + o(\Delta t), & j-1 \text{ and } j+1 \text{ did not adopt by time } t, \\ P_L\Delta t + o(\Delta t), & j-1 \text{ has adopted by time } t, \text{ and } j+1 \text{ has not}, \\ P_R\Delta t + o(\Delta t), & j+1 \text{ has adopted by time } t, \text{ and } j-1 \text{ has not}, \\ P_2\Delta t + o(\Delta t), & \text{both } j-1 \text{ and } j+1 \text{ have adopted by time } t, \end{cases} \tag{19a}$$

as $\Delta t \to 0$, where[1]

$$P_0 = p, \qquad P_L = p + q_L, \qquad P_R = p + q_R, \qquad P_2 = p + q_R + q_L. \tag{19b}$$

We now show that the expected fraction of adopters in the two-sided 1D model is the same as in the one-sided 1D model with $q = q_R + q_L$:

PROPOSITION 3. *The expected fraction of adopters in the two-sided 1D model is given by equation* (6) *with* $q = q_R + q_L$.

Proof: see Section 3.2.

Therefore, it immediately follows that

PROPOSITION 4. *The expected fraction of adopters in the two-sided 1D model as* $M \to \infty$ *is given by equation* (7) *with* $q = q_R + q_L$.

The implications of this result will be discussed in Section 4.

3.1. Simulations

In Figure 5 we show the average of 10,000 agent-based simulations of the two-sided 1D model. For both $M = 10$ and $M = 40$, the average fraction of adopters is well approximated by the

Figure 5 Comparison of agent-based simulations of the two-sided 1D model, averaged over 10,000 runs (dashes) with the explicit expression (6) for a finite M (dots), and with the explicit expression (7) for an infinite population (solid). Here, $p = 0.01$, $q = 1.2$ and $\Delta t = 0.05$. (A) $M = 10$. Dashed and dotted lines are indistinguishable. (B) $M = 40$. The three lines are nearly indistinguishable.

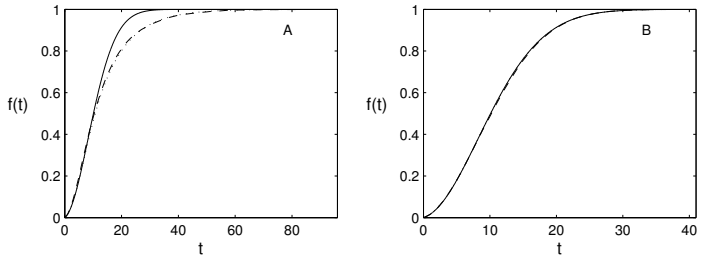

explicit expression (6) for a finite M. When $M = 10$, the average fraction of adopters is below the $M \to \infty$ limit, equation (7). However, already for $M = 40$, the average fraction of adopters is very close to the $M \to \infty$ limit. This shows that even for rather small populations, the expression (7) describes the growth of the two-sided 1D model very well. As in the one-sided case, as $M \to \infty$, the normalized variance of the process vanishes, and the $M \to \infty$ limit, equation (7), will match any simulation result, and not just the average over many simulations.

3.2. Proof of Proposition 3

The proof is similar to the one-sided case. The two-sided 1D model is also translation invariant, so the position of the anchor has no effect. We first note the following relations:

Lemma 6.

$$[IS_k] = [S_k] - [S_{k+1}]. \tag{20a}$$

$$[S_k I] = [S_k] - [S_{k+1}]. \tag{20b}$$

Proof. The configuration $(S_k) = (S_{k-1}\underline{S})$ may be written as a union of two disjoint configurations (or events) $(S_{k-1}\underline{S}) = (IS_{k-1}\underline{S}) \cup (SS_{k-1}\underline{S})$. Hence, its probability is the sum of the probabilities of the disjoint events: $[S_k] = [IS_k] + [S_{k+1}]$, which gives equation (20a). The configuration (S_k) can also be written as $(S_{k-1}\underline{S}) = (S_{k-1}\underline{S}I) \cup (S_{k-1}\underline{S}S)$, i.e. $[S_k] = [S_k I] + [S_{k+1}]$, which gives equation (20b). $\square$

LEMMA 7.

$$[IS_kI] = [S_k] - 2[S_{k+1}] + [S_{k+2}]. \tag{21}$$

Proof. The configuration $(IS_k) = (IS_{k-1}\underline{S})$ may be written as a union of two disjoint configurations (or events) $(IS_{k-1}\underline{S}) = (IS_{k-1}\underline{S}S) \cup (IS_{k-1}\underline{S}I)$. Hence, its probability is the sum of the probabilities of the disjoint events: $[IS_k] = [IS_{k+1}] + [IS_kI]$. Equation (21) then follows from Lemma 6. □

Using these lemmas we can write the master equations for $[S_k]$:

LEMMA 8. *The master equation for* $[S_k]$ *is:*

$$[\dot{S}_k] = \Big(-kp - q \Big)[S_k] + q[S_{k+1}], \qquad k = 1, \ldots, M-1. \tag{22}$$

Proof. We first consider the case $k = 1$. A configuration $(\underline{S})$ cannot be created. It is destroyed on the following occasions:

1. When $(S\underline{S}S)$ turns into $(S\underline{I}S)$ (with rate P_0).
2. When $(I\underline{S}S)$ turns into $(I\underline{I}S)$ (with rate P_L).
3. When $(S\underline{S}I)$ turns into $(S\underline{I}S)$ (with rate P_R).
4. When $(I\underline{S}I)$ turns into $(I\underline{I}I)$ (with rate P_2).

The master equation for $[S]$ is then

$$[\dot{S}] = -P_0[SSS] - P_L[ISS] - P_R[SSI] - P_2[ISI].$$

Using equation (19b), Lemma 3, Lemma 6 and Lemma 7, we get equation (22) for $k = 1$.

We now consider the case $k > 1$. A configuration $(S_{k-1}\underline{S})$ cannot be created. It is destroyed on the following occasions:

1. When $(SS_{k-2}\underline{S})$ turns into $(SS_lIS_r\underline{S})$ (with rate P_0, where $l = 0, 1, 2, \ldots, k-3$ and $r = k-3-l$).
2. When $(SS_{k-1}\underline{S})$ turns into $(SIS_{k-2}\underline{S})$ (with rate P_0).
3. When $(S_{k-1}\underline{S}S)$ turns into $(S_{k-1}\underline{I}S)$ (with rate P_0).

4. When $(IS_{k-1}\underline{S})$ turns into $(IIS_{k-2}\underline{S})$ (with rate P_L).

5. When $(S_{k-1}\underline{S}I)$ turns into $(S_{k-1}\underline{I}I)$ (with rate P_R).

The master equation for $[S_k]$ is therefore

$$[\dot{S_k}] = -(k-2)P_0[S_k] - 2P_0[S_{k+1}] - P_L[IS_k] - P_R[S_kI].$$

Using equation (19b), Lemma 3, Lemma 6 and Lemma 7 we get equation (22) for any $k > 1$. □

LEMMA 9. *The master equation for* $[S_M]$ *is:*

$$[\dot{S_M}] = -Mp[S_M]. \tag{23}$$

Proof. Same as for Lemma 5. □

Equation (22) and (23) show that the time evolution of $\{[S_k]\}_{k=1}^{M}$ is given by equation (17), i.e. the same system of equations as in the one-sided 1D model. As we have seen, the solution of these equations is given by equation (6).

4. Effective q

From Proposition 3 it follows, in particular, that:

COROLLARY 2. *For any given* p *and* M*, if* $q = q_R + q_L$*, then the expected fraction of adopters in the one-sided and in the two-sided 1D models are identical.*

Since in the one-sided model each individual influences a single "neighbor" with parameter q, while in the two-sided model he influences two "neighbors" with parameters q_L and q_R, this suggests that *the overall diffusion rate depends on the "sum" of the internal influences of each adopter on all its "neighbors".*

In order to motivate this finding, we note that for any cluster of adopters , only the two adopters at the two ends of the cluster can influence individuals who have not yet adopted (see Sections 9 and 13 for further discussion of the clusters-dynamics approach). Therefore, the expected adoption at the time interval $(t, t+\Delta t)$ due to internal influences is $k(t)(q_L + q_R)\Delta t$,

Figure 6 The effective q of individual j is $q_j^{\text{effective}} = q_{j,1} + q_{j,2} + q_{j,3} + q_{j,4}$.

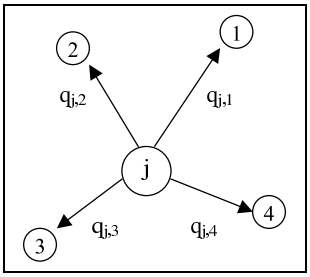

where $k(t)$ is the number of clusters. Hence, diffusion due to internal influences depends on $q_L + q_R$.

The result of Corollary 2 leads to the following definition (which is also valid for diffusion in models with a more complex spatial structure:)

DEFINITION 1. Let K_j be the number of neighbors of j, and let $q_{j,i}$ $(1 \le i \le K_j)$ be the influence parameter of j on its neighbor i. Then, the *effective* q of individual j is

$$q_j^{\text{effective}} = \sum_{i=1}^{K_j} q_{j,i}.$$

A typical case of an effective q is depicted in Figure 6.

Thus, Corollary 2 shows that when the values of M, p and $q^{\text{effective}}$ are the same in the one-sided and two-sided 1D models, the aggregate adoption dynamics is identical in the two models.

5. The fully-connected model

So far, we considered 1D models in which each individual is connected to his two nearest neighbors. We now consider the other extreme, the fully-connected model,see Figure 1, in which each individual can communicate with all the other $M-1$ individuals. We assume that the adoption probability of individual j which has not yet adopted is

$$\text{Prob}\{j \text{ adopts in } (t, t+\Delta t)\} = [p + \frac{q}{M-1} \cdot n(t)]\Delta t + o(\Delta t), \tag{24}$$

as $\Delta t \to 0$, where $n(t)$ is the number of adopters . Note that the internal influence parameter q has been divided by $M-1$, the total number of neighbors, in order to have the same $q^{\text{effective}}$ as in the 1D models.

Figure 7 Comparison of a single agent-based simulation of the fully-connected model with $M = 10^5$ (dashes), with the solution of the Bass model (solid). Here, $p = 0.01$, $q = 0.6$ and $\Delta t = 0.05$. The two lines are nearly indistinguishable.

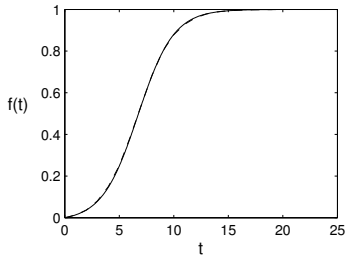

Let us denote by $\overline{f}(t)$ the solution of the deterministic equation

$$\frac{\mathrm{d}\overline{f}(t)}{\mathrm{d}t} = [1 - \overline{f}(t)][p + q\overline{f}(t)], \qquad \overline{f}(0) = 0, \tag{25}$$

which is the Bass model (1), rewritten for the fraction of adopters. In this case, it follows from Niu (2002) that

$$\lim_{M\to\infty} f(t) = \overline{f}(t). \tag{26}$$

Therefore,

COROLLARY 3. *The Bass model can be viewed as the $M \to \infty$ limit of the Fully-Connected model.*

To illustrate this result, in Figure 7 we compare the solution of the Bass model (25) with a single agent-based simulation of the fully-connected model with $M = 10^5$. As expected, the two lines are nearly indistinguishable.

6. Comparison of the 1D models with the Bass model

In Section 4 we saw that the adoption curve in the 1D models depends only on the values of p and $q^{\text{effective}}$. Therefore, it is natural to ask whether the Bass model with the same values of p and $q^{\text{effective}}$ would yield the same adoption curve. To answer this, we first note that when $q = 0$,

$$f_{1\text{D}}(t) \equiv f_{\text{Bass}}(t) = 1 - e^{-pt},$$

i.e., the adoption curve in the two models in identical. Indeed, the difference between the two models is due to internal influences, which do not exist when $q=0$. Once we allow for internal influences, however, the adoption levels in the two models increase. Therefore,

$$f_{1\mathrm{D}}(t) > 1 - e^{-pt}, \quad f_{\mathrm{Bass}}(t) > 1 - e^{-pt}, \qquad t > 0, \quad q > 0. \tag{27}$$

Moreover, for any $t>0$, the adoption level in the Bass model is higher than in the 1D model:

LEMMA 10. *For any $p>0$, $q>0$ and $t>0$,*

$$f_{1\mathrm{D}}(t) < f_{\mathrm{Bass}}(t). \tag{28}$$

Proof. See Appendix A. □

The role of the spatial structure in diffusion models is of most interest for products that are predominantly adopted through internal influences, i.e., when $p \ll q$ (see Section 8). In this case, one can quantify the aggregate adoption rate in the 1D model and in the Bass model as follows:

LEMMA 11. *Let $T_{1\mathrm{D}}$ and T_{Bass} denote the time for half of the population to adopt in the 1D model and in the Bass model, respectively. If $p \ll q$, then*

$$T_{1\mathrm{D}} \sim \frac{\sqrt{2\log 2}}{\sqrt{pq}}, \qquad T_{\mathrm{Bass}} \sim \frac{\log(q/p)}{q}.$$

Proof. Let $0 \le t \ll 1/p$. Then, a Taylor expansion of relation (3) gives

$$f_{1D} \sim 1 - e^{-pt - pqt^2/2} \sim 1 - e^{-pqt^2/2}. \tag{29}$$

Therefore, $T_{1\mathrm{D}} \sim \sqrt{2\log 2}/\sqrt{pq}$. Note that since $T_{1\mathrm{D}} \ll 1/p$, the validity of the Taylor expansion is a posteriori justified.

In the Bass model, the time for half of the population to adopt can be calculated directly from relation (2), yielding

$$T_{\mathrm{Bass}} = \frac{\log(2+q/p)}{p+q}.$$

Therefore, the result follows. □

Lemma 11 shows that the adoption level in the Bass model is considerably higher than in the 1D model, and that the difference between the two models increases with q/p:

COROLLARY 4. *If* $p \ll q$, *then*

1. $T_{\mathrm{1D}} \gg T_{\mathrm{Bass}}$.
2. *The ratio* $T_{\mathrm{1D}}/T_{\mathrm{Bass}}$ *is monotonically increasing in* q/p. *In particular,*

$$\lim_{q/p\to\infty} \frac{T_{\mathrm{1D}}}{T_{\mathrm{Bass}}} = \infty.$$

Proof. From Lemma 11 we have that

$$\frac{T_{\mathrm{1D}}}{T_{\mathrm{Bass}}} \sim \sqrt{2\log 2}\frac{\sqrt{q/p}}{\log(q/p)}.$$

Therefore, the results follow. □

Figure 8 shows a comparison of the adoption curves in the Bass model and in the 1D model with the same values of p and q. In accordance with Lemma 10, the adoption level in the Bass model is higher than in the 1D model. In addition, in accordance with Corollary 4, the difference between the Bass model and the 1D model increases with q/p.

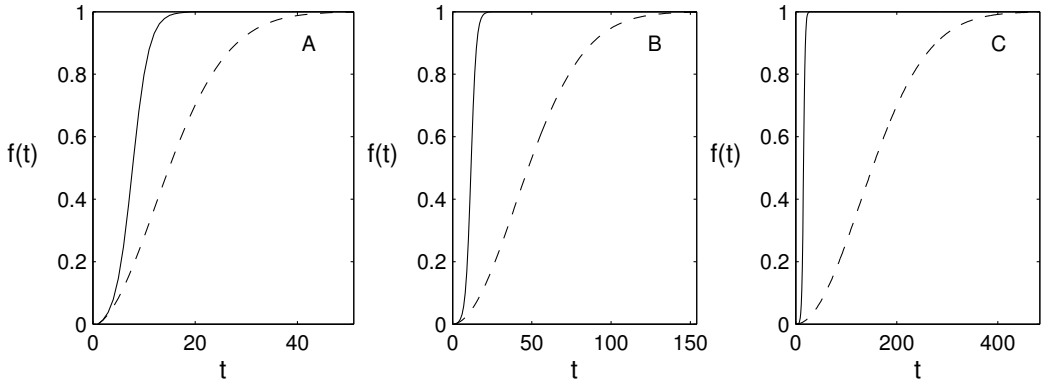

Figure 8 Fractional adoption in the Bass model (equation (1), solid) and in the 1D model (equation (7), dashes), for $q = 0.6$ and (A) $p = 0.01$, (B) $p = 0.001$, (C) $p = 0.0001$.

6.1. Mean-Field Approximation

In many cellular-automata models, it is not easy to solve, or even just to write explicitly, the master equations for all the possible configurations. Indeed, this is the reason why we did not extend the analysis of diffusion in the 1D models (see Sections 2.2 and 3.2) to multi-dimensional grids. In such cases, a common approach is to write the master equations only for the small configurations, and close the system using the *mean-field approximation*, i.e., the assumption that the state of each individual is independent of the state of its neighbors.

For example, under the mean-field approximation, we can approximate the probabilities in equation (11) of the 1D model as

$$[SS] \approx [S][S], \quad [IS] \approx [I][S].$$

Under these approximations, the master equation (11) can be replaced with

$$[\dot{I}] \approx P_0[S][S] + P_1[I][S], \quad [I]_{|t=0} = 0.$$

Since $[I] + [S] = 1$, we have

$$[\dot{I}] \approx P_0(1-[I])^2 + P_1[I](1-[I]), \quad [I]_{|t=0} = 0. \tag{30}$$

Substituting $P_0 = p$ and $P_1 = p+q$ in equation (30) yields

$$[\dot{I}] \approx (1-[I])\Big(p(1-[I]) + (p+q)[I]\Big) = (1-[I])(p+q[I]). \tag{31}$$

This equation is identical to equation (51) which governs the Bass model. Therefore, we conclude that

LEMMA 12. *The Bass model is a mean-field approximation of the 1D model.*

Since the results of these two models are very different (see Corollary 4 and Figure 8), this shows that the mean-field approximation can lead to very inaccurate results.

7. The lower-bound and upper-bound conjecture

The one-dimensional model and the fully-connected Bass model can be viewed as the least-connected and most-connected spatial models, respectively. From this perspective, any other spatial structure "lies between" these two cases. Therefore, the diffusion in any spatial structure can be expected to be faster than in the 1D model, and slower than in the Bass model:

CONJECTURE 1. *Let $f(t)$ be the expected fractional adoption rate in a spatial model with given p and $q^{effective}=q$. Then, $f(t)$ can be bounded from below and from above by*

$$f_{1\mathrm{D}}(t) \le f(t) \le f_{\mathrm{Bass}}(t). \tag{32}$$

In particular, as $M \longrightarrow \infty$,

$$1-e^{-(p+q)t+q\frac{1-e^{-pt}}{p}} \le f(t) \le \frac{1-e^{-(p+q)t}}{1+\frac{q}{p}e^{-(p+q)t}}. \tag{33}$$

A rigorous proof of Conjecture 1 is beyond the scope of this study. In order to begin to address this problem analytically, we first show in Section 8 that it is "enough" to prove Conjecture 1 for $q/p \gg 1$, rather than for any $p>0$ and $q>0$. Then, in Section 9 we introduce a clusters-dynamics approach, and use it to approximate the adoption curve $f(t)$ in D-dimensional Cartesian grids. The clusters-dynamics approximation shows that as D increases, the adoption becomes faster, but that it remains slower than in the Bass model (Section 10), thereby showing that Conjecture 1 holds for Cartesian grids of any dimension. In Section 11 we show that the addition of a small-world randomness has a minor effect of the diffusion curve. Hence, Conjecture 1 also holds for D-dimensional Cartesian grids with a small-world structure.

Assuming that Conjecture 1 is correct, then it provides the "maximal possible deviation" of the actual adoption curve from that of the Bass model. Indeed, there are various empirical findings that are inconsistent with the Bass model. For example, in the Bass model, $f'(t)$ is symmetric with respect to its maximum, see Figure 9A. However, empirical data shows that $f'(t)$ can be asymmetric (Mahajan, Muller and Bass 1993). Easingwood, Mahajan and Muller (1983)

Figure 9 $f'(t)$ as a function of t for $p=0.01$ and $q=0.6$. (A) The Bass model. (B) The 1D model.

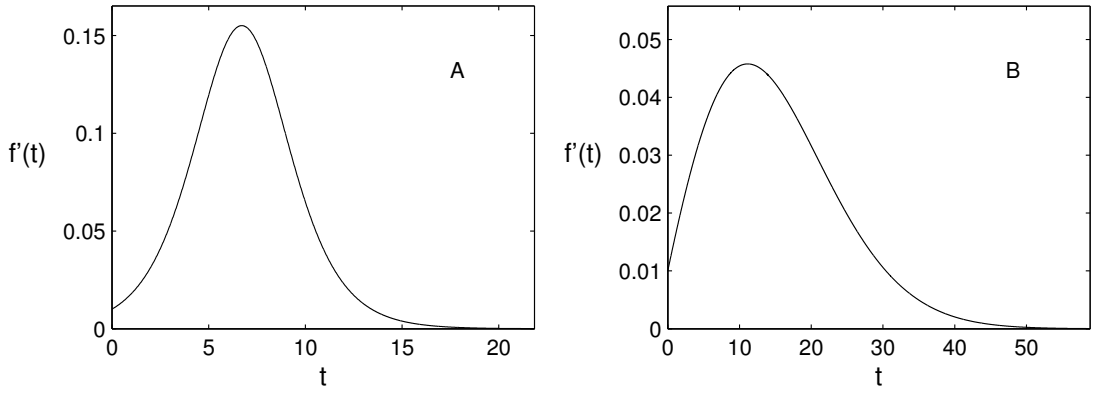

suggested that this asymmetry may be the result of a time-varying impact of the word-of-mouth effect. This study shows that some of the asymmetry may be due to the spatial structure. Indeed, Figure 9B shows that in the 1D model, $f'(t)$ is highly asymmetric with respect to its peak.

8. Parameter reduction using dimensional analysis

Consider a spatial diffusion model with parameters p and $q^{\text{effective}}=q$. We now use an applied mathematics technique, known as *dimensional analysis*, to show that the diffusion process depends on the *single* non-dimensional parameter q/p. For an introduction to dimensional analysis, see e.g., Chapter 6 in Lin and Segel (1988).

Let $\tilde{t}=pt$. Then, the external and internal adoption parameters, measured in the $\tilde{t}$ time-variable, are $\tilde{p}=p/p=1$ and $\tilde{q}=q/p$. Therefore, the function $f(\tilde{t})$ depends on the *single* parameter $\tilde{q}$, i.e.,

$$f(t;p,q)=g(\tilde{t};\tilde{q}),$$

where g is some unknown function. For example, in the Bass model and in the 1D model,

$$g_{\text{Bass}}(\tilde{t};\tilde{q})=\frac{1-e^{-(1+\tilde{q})\tilde{t}}}{1+\tilde{q}e^{-(1+\tilde{q})\tilde{t}}}, \qquad g_{\text{1D}}(\tilde{t};\tilde{q})=1-e^{-(1+\tilde{q})\tilde{t}+\tilde{q}(1-e^{-\tilde{t}})},$$

see equations (2) and (3), respectively.

The parameter q/p is dimensionless, and it expresses the ratio of external and internal influences. Thus, when $q/p \ll 1$, most adoptions occur through external adoptions, whereas when

$q/p \gg 1$, most adoptions occur through internal adoptions. Obviously, analyzing the role of the spatial structure in diffusion models is of most interest in the latter case, i.e., when $q \gg p$. Therefore, in what follows, we focus on this regime.

The above dimensional analysis shows that it is "enough" to prove Conjecture 1 for $q/p \gg 1$, rather than for any $p > 0$ and $q > 0$. Another application of this observation is as follows. In Section 9 we will derive a clusters-dynamics approximation for $f(t)$. In principle, a numerical verification of this approximation should be carried out over the two-dimensional parameter space $p > 0$ and $q > 0$. The above dimensional analysis implies, however, that it is enough to test the validity of this approximation over the one-dimensional parameter space $\tilde{q} > 0$, and even just for $\tilde{q} \gg 1$.

9. Clusters-dynamics analysis

In Sections 2 and 3 we derived an explicit expression for the expected fractional adoption curve $f(t)$ in one-dimensional grids. Unfortunately, it is not clear whether this approach can be extended to higher dimensions. In addition, this approach does not provide any insight as to the way in which the diffusion process progresses. Therefore, in what follows, we present a different analytic approach to this problem. While this method only provides an approximation for $f(t)$, it has the advantages that it is intuitive, and that it can be extended to higher dimensions (Sections 9.2 and 9.3), as well as to grids with a small-world structure (Section 11) and to models with heterogeneous individuals (Section 12).

9.1. One dimension

Let us define a *cluster of adopters* as a maximal group of connected adopters. We can "visualize" the diffusion process as follows:

1. A random creation of external adopters (seeds).
2. Each external adopter (seed) expands into a cluster of adopters through internal influences.
3. As clusters expand, they can merge into larger clusters.

We now construct the corresponding mathematical model. The rate at which new seeds are created is equal to $p(M-n(t))$. In the 1D model, for any cluster, only the two individuals at its two ends can influence non-adopters. Therefore, regardless of the cluster size, the expected increase in the cluster size between t and $t+\Delta t$ is $q\Delta t$.

The main issue is how to incorporate the effect of clusters merging into the model. Let us first assume that the effect of clusters merging can be neglected. Then, the fractional number of adopters satisfies the equation

$$f(t) \sim \int_0^t p(1-f(\tau))(1+q(t-\tau))\,d\tau, \tag{34}$$

where $p(1-f(\tau)) = p(M-n(\tau))/M$ is the fractional rate of new external adopters at time τ, and $(1+q(t-\tau))$ is the number of adopters in a cluster which was 'born' at time τ. This integral equation can be solved explicitly (see Appendix B), yielding

$$f(t) \sim 1 - e^{-pt/2}\left(\cos(yt) - \frac{p}{2}\frac{\sin(yt)}{y}\right), \qquad y = \sqrt{pq - p^2/4}. \tag{35}$$

In Figure 10 we compare the approximation (35) with the exact expression given by equation (3). As expected, this approximation is in good agreement with the exact expression during the initial phase of the diffusion, where the probability for clusters merging is small. As the adoption level increases, the probability of clusters merging increases, hence the accuracy of the approximation (35) deteriorates. At these high adoption levels the approximation (35) provides a significant overestimate, because it neglects the reduction in the number of clusters, hence in the number of new internal adoptions, as a result of clusters merging.

In order to incorporate clusters merging into the model, it is conceptually useful to allow clusters to overlap with each other, and to allow new clusters to form both inside and outside the existing clusters. Indeed, under this description,

1. The expected rate of new seeds (clusters) is constant, and is equal to $1/Mp$.

2. The probability $P(t) = 1-f(t)$ that a given person has *not* adopted by time t, is equal to the product of the probabilities that that person does not belong to any of the existing clusters,

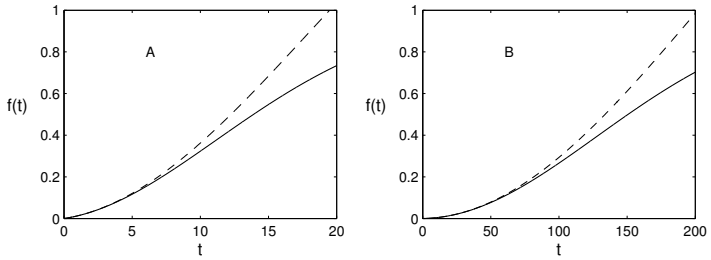

Figure 10 Fractional adoption in a 1D model with $q = 0.6$ and with A) $p = 0.01$ and B) $p = 0.0001$. The approximation (35) which neglects clusters merging (dashed line) is in good agreement with the exact expression (equation (3), solid line) during the early adoption state, but provides a significant overestimate afterwards.

since these probabilities are independent. Since the probability that a given person belongs to a cluster of size m_j is m_j/M, we have that

$$P(t) = \prod_{j=1}^{k(t)} \big(1 - \frac{m_j}{M}\big),$$

where $k(t)$ is the number of clusters .

To simplify the calculations, we assume that at each $\Delta t_p = 1/Mp$ time-step, exactly one new cluster is formed, and that once a new cluster appears, it expands at a constant rate of q.

We now calculate the number of adopters under the above assumptions:

- At time $t = 0$, there are no adopters. Therefore, $P(t = 0) = 1$.
- At time $t = \Delta t_p$, there is a single cluster of size 1. Therefore,$P(t = \Delta t_p) = 1 - 1/M$.
- At time $t = 2\Delta t_p$ the size of the first cluster is $1 + q\Delta t_p$ and the size of the second cluster is 1. Therefore,

$$P(t = 2\Delta t_p) = \big(1 - \frac{1 + q\Delta t_p}{M}\big) \cdot \big(1 - \frac{1}{M}\big).$$

- At time $t = k\Delta t_p$, there are k clusters of sizes $\{1 + (k-1)q\Delta t_p,\ 1 + (k-2)q\Delta t_p,\ \ldots,\ 1\}$. Therefore,

$$P(t = k\Delta t_p) = \prod_{j=0}^{k-1} \big(1 - \frac{1 + jq\Delta t_p}{M}\big). \tag{36}$$

From equation (36) we have that

$$\log P(t = k\Delta t_p) = \sum_{j=0}^{k-1} \log \big(1 - \frac{1 + jq\Delta t_p}{M}\big).$$

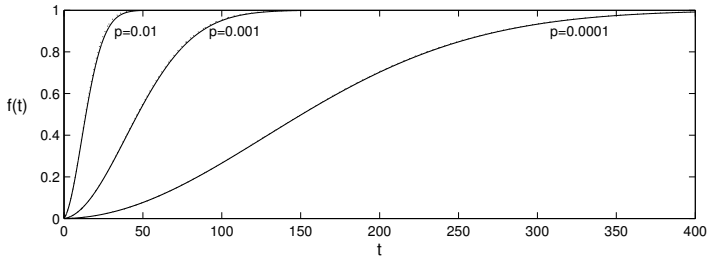

Figure 11 Fractional adoption in a 1D model with $q = 0.6$, and with $p = 0.01$ (left), $p = 0.001$ (center), and $p = 0.0001$ (right). Solid lines are the exact expression (3). Dashed lines are the clusters-dynamics approximation (37). In all three cases, the solid and dashed lines are nearly indistinguishable.

In addition, from the definitions of Δt_p and $t = k\Delta t_p$ we have that $k = Mpt$. Since each cluster only contains a small fraction of the population, we can use the approximation $\log(1-x) \approx -x$ to get,

$$\log P(t = k\Delta t_p) \sim -\sum_{j=0}^{k-1} \left(\frac{1 + jq\Delta t_p}{M}\right) = -\frac{k}{M} - \frac{k(k-1)}{2}\frac{q\Delta t_p}{M} \sim -\frac{k}{M} - \frac{k^2}{2}\frac{q\Delta t_p}{M} = -pt - qpt^2/2.$$

Therefore, $P(t) \sim e^{-pt-qpt^2/2}$, and

$$f_{1\mathrm{D}}(t) = 1 - P(t) \sim 1 - e^{-pt-qpt^2/2}. \tag{37}$$

The clusters-dynamics approximation (37) agrees with the Taylor approximation of the exact expression, see equation (29). Indeed, in Figure 11 we see that there is an excellent agreement between the clusters-dynamics approximation (37) and the exact expression (3). In particular, unlike approximation (35) which neglects clusters merging, see Figure 10, the excellent agreement between the clusters-dynamics approximation (37) and the exact expression (3) is maintained throughout the adoption process.

9.2. Two dimensions

Let us consider a 2D model in which the population is laid on a rectangular grid (with toroidal boundary conditions), and each member of the population is able to communicate with his four nearest neighbors, see Figure 12. The adoption probability of each individual which has not yet adopted is

$$\mathrm{Prob}\{j \text{ adopts in } (t, t+\Delta t)\} = [p + \frac{q}{4} \cdot A_j(t)]\Delta t + o(\Delta t), \tag{38}$$

Figure 12 The 2D model. Each individual is able to communicate with his 4 nearest neighbors.

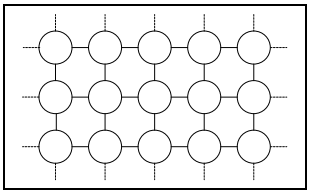

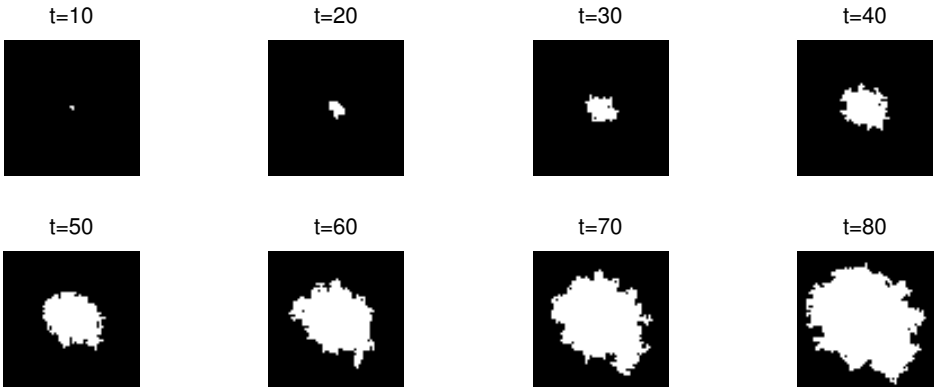

Figure 13 Expansion of a single cluster whose seed was generated at $t=0$, in an agent-based simulation of the 2D model with $q=0.6$.

as $\Delta t \to 0$, where $A_j(t)$ is the number of neighbors of j that adopted by time t. Note that the influence parameter of each neighbor is $q/4$, in order to have the same $q^{\text{effective}}$ as in the 1D models (see Section 4).

We now apply the clusters-dynamics approach to the 2D case. As in the 1D case, cluster seeds are randomly generated, and then they expand (and merge) with time. The analysis is considerably more complex, however, since the expansion rate of a two-dimensional cluster is not constant, but rather increases with its size m_j. Moreover, even for a given cluster size, the expansion rate depends on its shape. More precisely, a cluster expands at the rate of

$$m_j'(t) = l_j(t)q/4, \tag{39}$$

where l_j is the length of the cluster circumference, i.e., the number of non-adopters that are nearest-neighbors of the cluster.

It may thus seem that in order to implement the clusters dynamics approach, one needs to keep track of all possible 2D cluster configurations, which is a formidable task. The analysis

can be considerably simplified, however, if one notes that clusters tend on average to expand as squares, which later turn into circles (see e.g., Figure 13 and also (Wolf 1987, Evans 1993)). Therefore, the cluster circumference l_j scales as $\sqrt{m_j}$. Hence, the cluster growth rate $m_j'(t)$, see equation (39) scales as $\sqrt{m_j}q$. In other words, the radius of the square/circle increases linearly in time. Therefore, we can make the simplifying assumption that the number of adopters in a cluster can be approximated with

$$m_j(t) \approx 1 + (c_2 q(t - t_j))^2, \tag{40}$$

where t_j is the time at which the cluster was 'born', and c_2 is a constant.

Proceeding as in the 1D case, see equation (36), we have that

$$P(t = k\Delta t_p) = \prod_{j=0}^{k-1} \big(1 - \frac{1 + (jc_2 q\Delta t_p)^2}{M}\big). \tag{41}$$

Hence,

$$\begin{aligned} \log P(k\Delta t_p) &\approx -\sum_{j=1}^{k} \big(\frac{1 + (jc_2 q\Delta t_p)^2}{M}\big) = -\frac{k}{M} - \frac{(k-1)k(2k-1)}{6}\frac{(c_2 q\Delta t_p)^2}{M} \\ &\approx -\frac{k}{M} - \frac{k^3}{3}\frac{(c_2 q\Delta t_p)^2}{M} = -pt - (c_2 q)^2 pt^3/3. \end{aligned}$$

Therefore,

$$P(t) \approx e^{-pt - c_2^2 q^2 pt^3/3},$$

and

$$f_{2\mathrm{D}}(t) = 1 - P(t) \approx 1 - e^{-pt - c_2^2 q^2 pt^3/3}. \tag{42}$$

In Figure 14 we compare the 2D clusters-dynamics approximation (42) with $c_2 = 0.8$, with the average of 10 cellular-automata simulations. The approximation is reasonably accurate as the non-dimensional parameter $\tilde{q} = q/p$ changes over two orders of magnitude ($60 \le \tilde{q} \le 6000$). It is not, however, as accurate as in the 1D case, see Figure 11. We note that the only difference between the derivations of the 1D and 2D clusters-dynamics approximations is that in the 1D case we used the exact expression for the expected rate of a cluster growth, whereas in the 2D case we used the approximation (40). Therefore, the approximation (40) is probably the main reason for the larger approximation error in the 2D case.

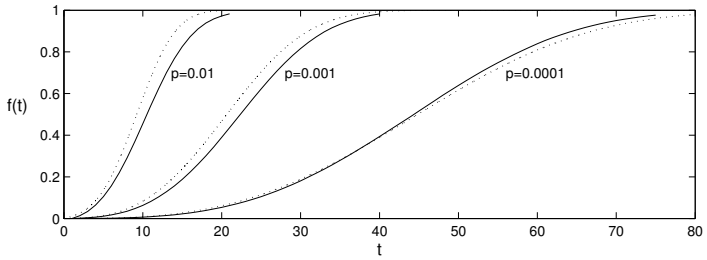

Figure 14 Fractional adoption in a 2D model with $q = 0.6$, and with $p = 0.01$ (left), $p = 0.001$ (center), and $p = 0.0001$ (right). Solid lines are averages over 10 cellular automata simulations, dashed lines are the clusters-dynamics approximation (42) with $c_2 = 0.8$.

9.3. Three and higher dimensions

In the 3D model the population is laid on a box grid (with toroidal boundary conditions), each member of the population is connected to his six nearest neighbors, and the overall adoption rate is

$$\text{Prob}\{j \text{ adopts in } (t, t+\Delta t)\} = [p + \frac{q}{6} \cdot A_j(t)]\Delta t + o(\Delta t), \tag{43}$$

as $\Delta t \to 0$, where $A_j(t)$ is the number of neighbors of j that adopted by time t. In this case, clusters expand on average as cubes, which later turn into spheres. Therefore, we make the assumption that

$$m_j(t) \approx 1 + (c_3 q(t - t_j))^3. \tag{44}$$

Hence, a similar derivation shows that

$$f_{3\text{D}}(t) \approx 1 - e^{-pt - c_3^3 q^3 p t^4/4}. \tag{45}$$

The extension to higher dimensions is similar.

In Figure 15 we compare the approximation (45) with the average of 10 cellular automata simulations. The approximation is reasonably accurate as the dimensionless parameter $\tilde{q} = q/p$ changes over two orders of magnitude ($60 \le \tilde{q} \le 6000$). It is, however, not as accurate as in the 2D case, see Figure 14. This is probably because the error introduced by the assumption that three-dimensional clusters expand as cubes/spheres, see equation (44), is larger than the one introduced by the assumption that two-dimensional clusters expand as squares/circles, see equation (40).

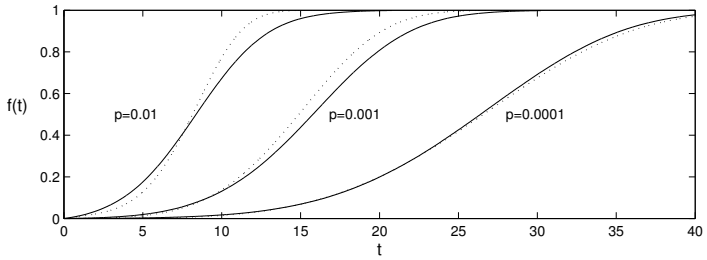

Figure 15 Fractional adoption in a 3D model with $q = 0.6$, and with either $p = 0.01$ (left), $p = 0.001$ (middle) or $p = 0.0001$ (right). Solid lines are averages over 10 cellular automata simulations with $M = 27000$, dashed lines are the clusters-dynamics approximation (45) with $c_3 = 0.635$.

10. Effect of grid dimensionality

In Section 9 we used the clusters-dynamics approach to show that when $p \ll q$, the adoption curve in a D-dimensional Cartesian grid can be approximated with

$$f_D(t) \sim 1 - e^{-pt(1 + a_D q^D t^D)},$$

where a_D is a constant which depends on D. Therefore, we have the following result:

LEMMA 13. *Consider the diffusion in a D-dimensional Cartesian grid with parameters p and $q_{\text{effective}} = q$. If $p \ll q$, the time for half of the population to become adopters scales as*

$$T_D \sim \frac{1}{(q^D p)^{1/(D+1)}}.$$

Thus,

$$T_{1\text{D}} \sim \frac{1}{(pq)^{1/2}}, \qquad T_{2\text{D}} \sim \frac{1}{(pq^2)^{1/3}}, \qquad T_{3\text{D}} \sim \frac{1}{(pq^3)^{1/4}}, \qquad \ldots,$$

Therefore, when $q \gg p$,

$$T_{1\text{D}} \gg T_{2\text{D}} \gg T_{3\text{D}} \gg \ldots$$

i.e., *the adoption-rate increases with the grid dimensionality.* In particular,

$$T_D < T_{1\text{D}}, \qquad D = 2, 3, \ldots \tag{46}$$

In addition, from Lemmas 11 and 13 it follows that

$$T_D > T_{\text{Bass}}, \qquad D = 1, 2, 3, \ldots \tag{47}$$

Figure 16 Comparison of a single agent-based simulation of the 1D model (solid), the 2D model (dash-dots), the 3D model (dots), and the fully-connected model (dashes). Here, $q=0.6$, $M=46,656$, $\Delta t=0.05$, and (A) $p=0.01$, (B) $p=0.0001$.

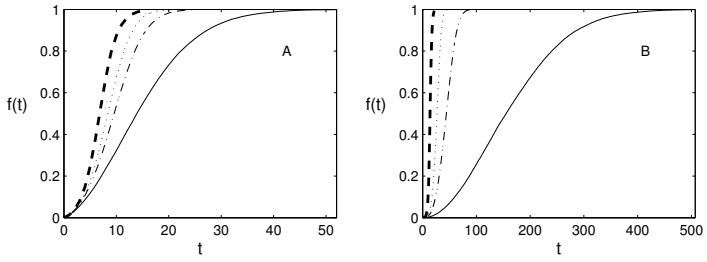

The above analysis would remain unchanged if we redefine T to be the time for any fraction of the population to become adopters. Therefore, grid dimensionality affects the entire adoption curve. Hence, relations (46) and (47) show that Conjecture 1 holds for Cartesian grids of any dimension. To see that, in Figure 16 we plot the adoption dynamics in agent-based simulations of the 1D, 2D, 3D and fully-connected models with $q^{\text{effective}}=0.6$, and with either $p=0.01$ or with $p=0.0001$. In both cases, the adoption becomes faster as D increases. Thus, the adoption in the 2D model is faster than in the 1D model, the adoption in the 3D model is even faster, and the fully-connected model is faster than all other models.

From Lemma 13 it follows that

$$\frac{T_{D+1}}{T_D} \sim \left(\frac{q}{p}\right)^{1/(D+1)(D+2)}. \tag{48}$$

Therefore, we conclude that *the relative increase in the adoption-rate decreases as D increases.* Indeed, in Figure 16 we see that the increase in the adoption rate between $D=1$ and $D=2$ is significantly larger than the increase between $D=2$ and $D=3$. Relation (48) also implies that *the relative increase in the adoption-rate increases as $\tilde{q}=q/p$ increases.* Indeed, the effect of the increasing dimension is more pronounced in Figure 16B where $q/p=6000$, than in Figure 16A where $q/p=60$.

11. Small-world networks

So far, we only considered populations with a deterministic Cartesian structure, in which there are no connections between non-adjacent neighbors. In 1998, Watts and Strogatz suggested

that social networks have a small-world structure, in which most connections are local, but there are also some random long-range connections between non-adjacent neighbors (Watts and Strogatz 1998). Watts and Strogatz showed that the addition of a small fraction of long-range connections leads to a considerable reduction in the average distance between any two members of the population (the "six degrees of separation" concept), and that, as a result, diffusion progresses significantly faster than without these random connections.

We now use the clusters-dynamics approach that was developed in Section 9 to analyze the effect of a small-world structure in the diffusion models considered in this study. Clearly, the addition of long-range connections has no effect on the creation of new clusters. In addition, a small fraction of long-range connections has a minor effect on the expansion of a cluster. For example, if 1% of the individuals have long-range connections, then there is a probability of $0.99^{20} \approx 82\%$ that a cluster of 20 individuals will not feel the small-world structure. Therefore, we reach the surprising conclusion that *the addition of a small fraction of long-range connections has a minor effect on the fractional adoption curve.*

Why is it, then, that the small-world structure had such a large effect in the original 1998 paper of Watts and Strogatz? The answer is that in that study, adoption always started from a single adopter at $t = 0$ ("patient zero"), and then progressed only through internal influences. In that case, the key parameter is the average distance from the first adopter, which is highly sensitive to the addition of long-range connections. This is not the case, however, in the models considered in this study, where diffusion starts from numerous external adopters (which expand into numerous clusters), and not from a single adopter.

In order to illustrate numerically the effect of a small-world structure on the diffusion process, in Figure 17A we plot the fractional adoption curve in a two-dimensional network with and without 1% random links, with $p = 0.001$, $q = 0.6$, $M = 10,000$ and zero adopters at $t = 0$. As predicted by the clusters-dynamics approach, the two adoption curves are nearly identical. In Figure 17B we plot the fractional adoption curve in a two-dimensional network, using the same random grid structure as in Figure 17A with $q = 0.6$ and $M = 10,000$, but with a single

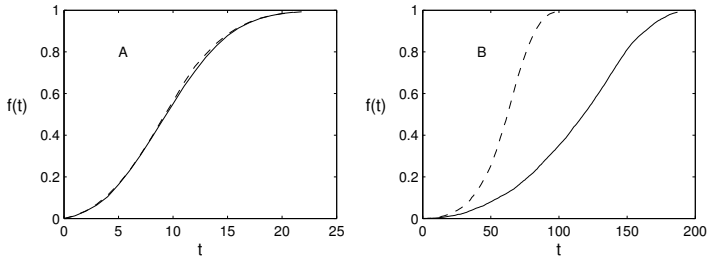

Figure 17 Agent-based simulation of the adoption in a two-dimensional network with (dashed line) and without (solid line) 1% random links. In all simulations, $q = 0.6$ and $M = 10,000$. A: $p = 0.001$ and no adopters at $t = 0$. B: $p = 0$ and a single adopter at $t = 0$.

adopter at $t = 0$ and with no subsequent external adoptions (i.e., $p = 0$ for $t > 0$). In that case, the addition of 1% random links indeed has a large effect on the diffusion curve, in agreement with Watts and Strogatz (1998). Finally, we note that we repeated the simulations of Figure 17 with a one-dimensional network, with and without 1% random links, and obtained similar results (data not shown).

12. Effect of heterogeneity

So far, we only considered agent-based models in which all individuals have the same p and q. Since individuals are more likely to be heterogeneous, an important question is whether our results will remain "the same" if we allow for heterogeneity in the values of p and q among individuals.

Goldenberg, Libai and Muller (2001) studied numerically the effect of heterogeneity in p and q in the fully-connected agent-based model. Their simulations showed that heterogeneity has a minor effect on the diffusion. This result can be explained as follows. The expected rate of new external adopters depends on the average of p among the individuals who have not yet adopted. Therefore, heterogeneity in p should have no effect on the rate of new external adopters. Similarly, the expected rate of new internal adopters depends on the cumulative effect of the internal influences of all the adopters. Therefore, the expected rate of new internal adopters depends on the average of q. Hence, heterogeneity in q should have no effect on the rate of new external adopters.

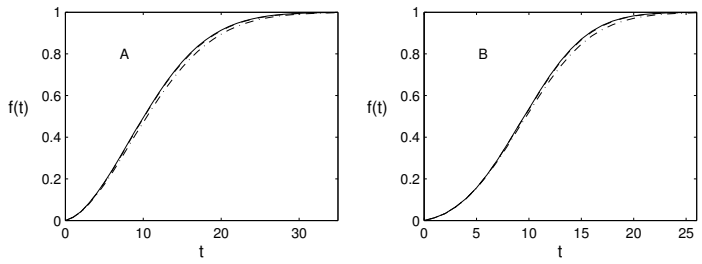

Figure 18 The aggregate adoption dynamics in agent-based simulations: A Comparison between the cases of homogeneous and heterogeneous individuals. Solid line corresponds to homogeneous individuals with $p = \bar{p}$ and $q = \bar{q}$, where $\bar{p} = 0.01$ and $\bar{q} = 0.6$. Dashed line corresponds to heterogeneous individuals with values of p and q that are uniformly drawn from $[0.8\bar{p},\ 1.2\bar{p}]$ and $[0.8\bar{q},\ 1.2\bar{q}]$, respectively. Dashed and solid lines are nearly indistinguishable. Dash-dot line corresponds to heterogeneous individuals with values of p and q that are uniformly drawn from $[0.5\bar{p},\ 1.5\bar{p}]$ and $[0.5\bar{q},\ 1.5\bar{q}]$, respectively. In all simulations $M = 1,000,000$ and $\Delta t = 0.05$. A: 1D simulations. B: 2D simulations. .

The cluster-dynamics approach allows us to analyze the effect of heterogeneity in p and q in agent-based models with a spatial structure. Since external adoptions are independent of the spatial structure, heterogeneity in p should have no effect on the rate of new external adopters. Similarly, the expansion rate of a cluster depends on the cumulative effect of the internal influences of all the adopters on the boundary of the cluster. Therefore, heterogeneity in q should only have a minor effect on the rate of new external adopters.

In order to confirm this prediction, in Figure 18 we compare the aggregate adoption curve with homogeneous individuals, to the adoption curve with heterogeneous individuals, in 1D and 2D agent-based simulations. When the values of p and q of the heterogeneous individuals are uniformly distributed within $\pm 20\%$ of the corresponding values of the homogeneous individuals, the two curves are nearly indistinguishable. As we further increase the heterogeneity level to $\pm 50\%$, the two curves are not identical, but are still very close. These simulations thus confirm the clusters-dynamics prediction that heterogeneity in p and q can only have a minor effect, if at all, on the aggregate diffusion dynamics.

13. Discussion - the effect of the spatial structure

The overall goal of this study has been to gain insight into the effect of the spatial structure on the diffusion of new products. We saw that it is useful to visualize the diffusion process as the combination of two separate processes: Random creation of external adopters, followed up by the expansion of each external adopter into a cluster of adopters through internal influences. Since the creation of new clusters is independent of the spatial structure, the spatial structure affects the diffusion only through its effect on the expansion of clusters.

The clusters-dynamics method provides a unified approach for explaining the various findings of this study:

1. In Section 4 we proved that in the two-sided 1D models, the diffusion depends only on $q^{\text{effective}} = q_R + q_L$. Indeed, this is because the expansion rate of a 1D cluster depends on the sum of the internal influences of the adopters at the two sides of the cluster.

2. In Section 10 we saw that increasing the dimension of the grid leads to a faster diffusion. In order to explain this observation, we note that clusters expand via the internal influences of the adopters located on the boundary of the cluster, since only the "boundary adopters" can influence non-adopters. For a given cluster size, as we increase the dimension, the average number of adopters at the cluster boundary increases. Therefore, the expansion rate of the cluster increases with the dimension.

3. In Section 11 we used the cluster-dynamics description to predict that a small-world structure has a minor effect on the aggregate diffusion dynamics, since it hardly affects the expansion rate of the clusters.

4. In Section 12 we used the cluster-dynamics description to explain why heterogeneity in p and q has a minor effect on the aggregate diffusion dynamics.

For a given population size, increasing the dimension reduces the average distance between individuals. Therefore, this provides an alternative explanation to the observation that increasing the dimension leads to a faster diffusion. If this explanation is correct, then the addition of

a small-world structure should have a large effect on the adoption curve. Our simulations show, however, that this is not the case. Indeed, the average distance between individuals is the key factor when there is a singe external adopter ("patient zero"), and all subsequent adoptions are internal. In product diffusion models, however, the population size M is large. Since the number of external adopters is proportional to M, adoption starts from numerous external adopters. Each of these external adopters then influences its neighbors, leading to the cluster-dynamics scenario of the diffusion process, rather than to a "patient-zero" single-cluster scenario.[2]

14. Final remarks

Agent-based models provide a powerful tool for studying the diffusion of new products. Until now, these models were used to compute the adoption curve numerically. In this study we introduced several analytical approaches to this problem: An explicit calculation of the adoption curve in the one-dimensional case, a cluster-dynamics approximation of the adoption curve in the multi-dimensional case, and a parameter reduction using dimensional analysis. The clusters-dynamics approach allowed us to better understand the effect of the spatial structure on the diffusion process, and to provide analytic support to the validity of Conjecture 1 that the diffusion rate is bounded from below by the Bass model and from above by the 1D model, for Cartesian grids with or without a small-world structure, and for either homogeneous or heterogeneous individuals.

This study raises several important questions which require further research. For example, what is the effect of a scale-free social network (Barabási and Albert 1999), or of other network structures, on the diffusion? Can the clusters-dynamics approximation be made more accurate, as well as more rigorous? Under which conditions does Conjecture 1 hold? What is the "correct" structure of social networks which is to be used in agent-based models of diffusion of new products?

Endnotes

1. For simplicity, we assume here that if both neighbors have already adopted then their combined influence is $q_L + q_R$. However, even if P_2 is different, it is possible to use our method to calculate explicitly the expected fraction of adopters (Gibori 2007).

2. This conclusion is consistent with the explicit expressions (2) and (3) for the fully-connected and 1D models, respectively. Indeed, these expressions show that as M increases, the fractional adoption curve $f(t)$ becomes independent of M. Therefore, for example, doubling the population size will double the number of external adopters.

Acknowledgments

We thank Boaz Nadler and Eitan Muller for useful discussions.

References

Alfrey, T. and Lloyd, W. G. (1963). "Kinetics of High-Polymer Reactions: Effects of Neighboring Groups". *The Journal Of Chemical Physics,* **38**, pp. 318-321.

Alkemade, F. and Castaldi, C. (2005). "Strategies for the Diffusion of Innovations on Social Networks". *Computational Economics,* **25**, pp. 3-23.

Barabási, Albert-László and Albert, Réka (1999). "Emergence of scaling in random networks". *Science,* **286**: pp. 509-512.

Bass, F.M. (1969). "A New Product Growth Model for Consumer Durables". *Management Science* **15**, pp. 215-227.

Bell, D. and Song, S. (2007), "Neighborhood Effects and Trial on the Internet: Evidence from Online Grocery Retailing". *Quantitative Marketing and Economics,* **5**, pp. 361-400.

Ben-Avraham, D. and Köhler, J. (1992), "Mean-Field (n,m)-Cluster Approximations for Lattice Models". *Physical Review A,* **45**, pp. 8358-8370.

Bonabeau, E. (2002). "Agent-Based Modeling: Methods and Techniques for Simulating Human Systems". *Proc. National Academy of Sciences,* **99**: pp. 7280-7287.

Bronnenberg, B. J. and Mela, C. F. (2004). "Market Roll-Out and Retailer Adoption for New Brands". *Marketing Science,* **23**: pp. 500-518.

Delre, S. A., Jager, W., Bijmolt, T. H. A. and Janssen, M. A. (2007), "Targeting and Timing Promotional Activities: An Agent-Based Model for the Takeoff of New Products". *Journal of Business Research,* **60**, pp. 826-835.

Easingwood, C. J., Mahajan, V. and Muller, E. (1983), "A Nonuniform Influence Innovation Diffusion Model of New Product Acceptance". *Marketing Science*, **2**, pp. 273-296.

Epstein, J. M. and Axtell, R. (1996). *Growing Artificial Societies: Social Science From the Bottom Up.* MIT Press/Brookings Institution.

Evans, J. W. (1993), "Random and Cooperative Sequential Adsorption". *Reviews of Modern Physics,* **65**, pp. 1281-1330.

Garber, T., Goldenberg, J., Libai, B. and Muller, E. (2004)"From Density to Destiny: Using Spatial Dimension of Sales Data for Early Prediction of New Product Success". *Marketing Science*, **23**, pp. 419428.

Gibori, R. (2007), "Analysis of Cellular Automata Diffusion Models in Marketing". M.Sc thesis, Tel Aviv University, Tel Aviv, Israel.

Gilbert, N. and Troitzsch, K. (2005). *Simulation for the Social Scientist*, Open University Press, 2nd edition.

Grimm, V. and Railsback, S. F. (2005). *Individual-based Modeling and Ecology*, Princeton University Press.

Goldenberg, J., Libai, B. and Muller, E. (2001) "Using Complex Systems Analysis to Advance Marketing Theory Development". *Academy of Marketing Science Review.* [Online] **01**, special issue on Emergent and Co-evolutionary Processes in Marketing.

Goldenberg, J., Libai, B. and Muller, E. (2001) "Riding the Saddle: How Cross-Market Communications Can Create a Major Slump in Sales". *Journal of Marketing*, **66**, pp. 1-16.

Goldenberg, J., Libai, B., Solomon, S., Jan, N. and Stauffer, D. (2000) "Marketing Percolation". *Physica A*, **284**, pp. 335-347.

Jackson, M. O. (2006). "The Economics of Social Networks". In Blundell, R., Newey, W., Persson, T. (Eds.), *Advances in Economics and Econometrics, Theory and Applications: Ninth World Congress of the Econometric Society.* Cambridge University Press, Cambridge: pp. 1-56.

Jackson, M.O. and Rogers, B.W. (2007) "Relating Network Structure to Diffusion Properties through Stochastic Dominance". *The B.E. Journal of Theoretical Economics* **7**, Article 6.

Keller, J. B. (1963), "Reaction Kinetics of a Long-Chain Molecule. II. Arends' Solution", *The Journal Of Chemical Physics,* **38**, pp. 325-326.

Kim, P., Lee, P., Levy, D., (2007) "Modeling Imatinib-Treated Chronic Myelogenous Leukemia: Reducing the Complexity of Agent-Based Models" *Bull Math Biol.* **70**, pp. 728-744.

Lin, C. C. and Segel, L.A (1988). *Mathematics Applied to Deterministic Problems in the Natural Sciences.* SIAM, Philadelphia

Mahajan, V., Muller, E. and Bass, F. M. (1993). "New-Product Diffusion Models". In J. Eliashberg and G. L. Lilien, editors, *Handbooks in Operations Research and Management Science*, Volume 5: Marketing, pp. 349-408. North-Holland, Amsterdam, The Netherlands.

Mahajan, V., Muller, E. and Bass, F. M. (1995). "Diffusion of new products: Empirical generalizations and managerial uses". *Management Science* **14**: pp. G79-G88.

Management Science **50** Number 12 Supplement, Dec 2004 ISSN 0025-1909: pp. 1833-1840.

Matsuda, H., Ogita, N., Sasaki, A. and Sato, K. (1992), "Statistical Mechanics of Population – The Lattice Lotka-Volterra Model". *Progress of Theoretical Physics* **88**: pp. 1035-1049.

López-Pintado, D. (2008). "Diffusion in Complex Social Networks". *Games and Economic Behavior* **62**: pp. 573-590.

Niu, S.C. (2002). "A Stochastic Formulation of the Bass Model of New-Product Diffusion". *Mathematical Problems in Engineering* **8**: pp. 249-263.

Pastor-Satorrás, R. and Vespignani, A. (2001). "Epidemic Spreading in Scale-Free Networks". *Physical Review Letters* **86**: pp. 3200-3203.

Samuelson, D. A. and Macal, C. M. (2006). "Agent-Based Modeling Comes of Age". *OR/MS Today* **33**: pp. 34-38.

Sinha, R. K. and Chandrashekaran, M. (1992). "A Split Hazard Model for Analyzing the Diffusion of Innovations." *Journal of Marketing Research* **29**: pp. 116-127.

Van den Bulte, C. and Lilien, G. L. (2001). "Medical Innovation Revisited: Social Contagion versus Marketing Effort". *American Journal of Sociology* **106**: pp. 1409-1435.

Vega-Redondo, F. (2006). *Complex Social Networks.* Econometric Society Monographs Series, Cambridge University Press, Cambridge.

Watts, D. J., and Strogatz, S. H. (1998). "Collective Dynamics of 'Small-world' Networks." *Nature* **393**: pp. 440-442.

Wolf, D. E. (1987). "Wulff construction and anisotropic surface properties of two-dimensional Eden clusters." *J Phys. A: Math. Gen.* **20**: pp. 1251-1258.

Appendix

A. Proof of Lemma 10

Since

$$f_{1\mathrm{D}} = 1 - e^{\Big(-(p+q)t + q\dfrac{1-e^{-pt}}{p}\Big)},$$

the adoption rate in the 1D model is given by

$$\dot{f}_{1\mathrm{D}}(t) = (1 - f_{1\mathrm{D}})[p + q(1 - e^{-pt})]. \tag{49}$$

Therefore, by equation (27), for any $q > 0$ and $t > 0$,

$$\dot{f}_{1\mathrm{D}}(t) < (1 - f_{1\mathrm{D}})(p + q f_{1\mathrm{D}}). \tag{50}$$

For comparison, the adoption rate in the Bass model is given by

$$\dot{f}_{\mathrm{Bass}}(t) = (1 - f_{\mathrm{Bass}})(p + q f_{\mathrm{Bass}}). \tag{51}$$

Equation (28) follows from explicit integration of equation (50). Indeed, from equation (50) we have that

$$\frac{\dot{f}_{1\mathrm{D}}}{(1 - f_{1\mathrm{D}})(p + q f_{1\mathrm{D}})} = \frac{\dot{f}_{1\mathrm{D}}}{p+q}\left(\frac{1}{1 - f_{1\mathrm{D}}} + \frac{q}{p + q f_{1\mathrm{D}}}\right) < 1.$$

Taking the integral between 0 and t gives

$$\frac{1}{p+q}\Big(-\ln(1 - f_{1\mathrm{D}}) + \ln(p + q f_{1\mathrm{D}})\Big)\Big|_0^t < t.$$

Since $f_{1\mathrm{D}}(0)=0$, we have that

$$\ln(p+qf_{1\mathrm{D}}(t))-\ln(1-f_{1\mathrm{D}}(t))-\ln p<t(p+q).$$

Therefore, $p+qf_{1\mathrm{D}}(t)<p(1-f_{1\mathrm{D}})e^{t(p+q)}$. Hence,

$$f_{1\mathrm{D}}(t)<\frac{1-e^{-(p+q)t}}{1+\frac{q}{p}e^{-(p+q)t}}=f_{\mathrm{Bass}}(t).$$

B. Proof of equation (35)

Let $f(t)$ be the solution of

$$f(t)=p\int_0^t(1-f(\tau))(1+q(t-\tau))\,d\tau. \tag{52}$$

and let $F(s)=\mathcal{L}(f(t))=\int_0^\infty f(t)e^{-st}\,dt$ be the Laplace transform of $f(t)$. Equation (52) can be rewritten as

$$f=p(1-f)\star(1+qt),$$

where $\star$ is the Laplace transform convolution. Therefore, if we take the Laplace transform of both sides and use the relation

$$\mathcal{L}(t^{k-1})=\frac{\Gamma(k)}{s^k},\qquad k>0,$$

we get that

$$F=p\left(\frac{1}{s}-F\right)\left(\frac{1}{s}+\frac{q}{s^2}\right).$$

Therefore,

$$F=\frac{p}{s}\frac{s+q}{s^2+ps+pq}.$$

In order to transform back, we first rewrite F as

$$F=\frac{p}{s}\frac{s+q}{(s-s_1)(s-s_2)},\qquad s_{1,2}=\frac{-p\pm\sqrt{p^2-4pq}}{2}. \tag{53}$$

Recall that

$$\mathcal{L}^{-1}\left(\frac{1}{(s-s_1)(s-s_2)}\right)=\frac{1}{s_1-s_2}\left(e^{s_1t}-e^{s_2t}\right),\quad \mathcal{L}^{-1}\left(\frac{s}{(s-s_1)(s-s_2)}\right)=\frac{1}{s_1-s_2}\left(s_1e^{s_1t}-s_2e^{s_2t}\right),$$

and

$$\mathcal{L}^{-1}\left(\frac{1}{s}G\right) = \int_0^t g(\tau)\,d\tau, \qquad G = \mathcal{L}(g).$$

Therefore, transforming equation (53) back gives

$$f = p\int_0^t \frac{1}{s_1 - s_2}\Big((s_1+q)e^{s_1\tau} - (s_2+q)e^{s_2\tau}\Big)\,d\tau.$$

Integrating the right-hand-side gives, after some technical calculations, the result.